Arch. Metall. Mater., Vol. 61 (2016), No 4, p. 2177–2182

DOI: 10.1515/amm-2016-0347

T. MOSKALEWICZ*,#, A. BABKIEWICZ*, B. DUBIEL*, M. KOT**, A. RADZISZEWSKA*, A. ŁUKASZCZYK***

POROUS SiO_2/HAp COATINGS ON Cp-TITANIUM GRADE 1 SURFACES PRODUCED BY ELECTROPHORETIC DEPOSITION

Porous hydroxyapatite doped SiO_2 coatings were electrophoretically deposited (EPD) on commercially pure titanium. The influence of EPD parameters on coatings quality was investigated. Microstructural observation was done using transmission and scanning electron microscopy as well as X-ray diffractometry.

The coatings consisted of spherical micro and nanocrystalline hydroxyapatite (HAp) as well as amorphous SiO_2 nanoparticles. The coatings exhibited open porosity with pore diameter up to 1 μm and due to presence of nanoparticles high surface development.

It was found that application of SiO_2/HAp coating increase corrosion resistance of titanium in Ringer's solution.

Keywords: titanium, porous coating, corrosion resistance, electrophoretic deposition

1. Introduction

Titanium is well known as one of the widely used metallic material for biomedical application. Commercially pure titanium (Cp-Ti) is an alternative material for AISI316L stainless steel and Co-Cr alloys due to its better biocompatibility and corrosion resistance [1,2]. However, in some biomedical applications e.g. hard tissue replacement, when high strength and good tribological properties are necessary, the Cp-Ti is unsuitable. Therefore its use in implants is restricted to applications which involve moderate mechanical stress, such as dental implants, preferentially for endosseous dental implant applications [3,4]. Such implants have direct contact with bone.

To improve the biological response to titanium, various surface engineering methods are applied. Presently, porous coatings deposited on titanium and its alloys have become an important aspect of biomaterials. Porous coatings for stabilization of implant are an alternative to bone cement fixation. Such coatings exhibit a three-dimensional interconnected array of pores, which allows bone tissue ingrowth [5]. It is very challenging to deposit a porous nanocrystalline HAp coating with controlled pore size and good adhesion to the substrate for dental implants [6]. High porosity is preferable especially for porous scaffold biomaterials [1]. However, high porosity decreased mechanical strength of porous coatings.

Bioceramics hydroxyapatite or tricalcium phosphate or bioactive glasses are known to as very important biocompatible and bioactive materials. After implantation of these bioceramics form a carbonated apatite (HCA) layer on their surfaces, which composition and structure is equivalent to the mineral phase of osseous tissue [7]. The unique properties of hydroxyapatite (excellent corrosion resistance, promoted bone cell attachment and bone formation) make them good candidates for many dental applications. Nanocrystalline HAp is more desirable than microcrystalline one because of its structural similarity with apatite [8]. Nanocrystalline particles may also contribute to better coating adhesion to the substrate.

The problems of compact porous ceramic implants are their poor mechanical properties, fracture toughness and load bearing capacity [9]. Also HAp ceramic, due to the poor mechanical properties, cannot be used for load bearing applications. The most important uses of HAp include bone graft substitutions and coatings on metallic implants. This problem is significantly reduced in the case of porous ceramic coating deposited on materials with good mechanical properties such as titanium and its alloys.

Many studies reported the importance of silica in bioactive materials for the bonding of bone [9,10]. Silica has three functions: (i) metabolic - to partake in cellular development and gene expression, (ii) chemical – as the nature of bonding to bone of bioglasses relates to the in vivo solubility of these glasses that in turn is a function of its silica content, (iii) mechanical – silica particles improve the strength of a hydroxyapatite coatings [9]. Therefore, amorphous silica particles was used in order to enhance hydroxyapatite in our coatings.

A very convenient method to deposit ceramic nano and micro particles is electrophoretic deposition (EPD) [11-13]. Electrophoretic deposition (EPD) is a two-step process. In the first step a charged particles in a stable colloidal suspension are

* AGH UNIVERSITY OF SCIENCE AND TECHNOLOGY, FACULTY OF METALS ENGINEERING AND INDUSTRIAL COMPUTER SCIENCE, 66 CZARNOWIEJSKA STR., 30-054 KRAKÓW, POLAND

** AGH UNIVERSITY OF SCIENCE AND TECHNOLOGY, FACULTY OF MECHANICAL ENGINEERING AND ROBOTICS, AL. A. MICKIEWICZA 30, 30-059 KRAKÓW, POLAND

*** AGH UNIVERSITY OF SCIENCE AND TECHNOLOGY, FACULTY OF FOUNDRY ENGINEERING, 23 REYMONTA STR., 30-059 KRAKÓW, POLAND

Corresponding author: tmoskale@agh.edu.pl

moved through the liquid due to electric field. In the second step the particles are deposited on an oppositely charged conductive substrate [12,13]. EPD enables production of a wide range of compact or porous nano and microstructures, from nanometric coatings up to 1 mm thick coatings. In the present work this method was selected to deposit porous HA/SiO_2 coatings on Cp-Titanium Grade 1. The main aim of this work was to elaborate the EPD conditions for application of good quality coatings and to characterize their microstructure, adhesion to the substrate and corrosion resistance in Ringer's solution.

2. Experimental

The samples (substrates) for the coating deposition were made from the Cp-Ti1 material with a chemical composition (in wt %) as follows: 0.03 C, 0.005 N, 0.001 H, 0.06 O, Ti balance. The material was delivered by Shanghai Huaxia Industry Co. Ltd, China. The microstructure of the Cp-Ti1 consisted of α (hexagonal close-packed) phase. The grain diameter was in the range of 10 μm – 70 μm (Fig. 1). In some grains an annealing twins were occurred.

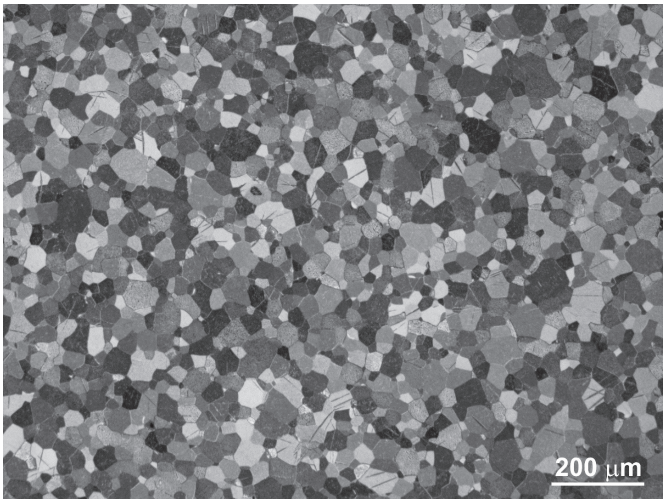

Fig. 1. Microstructure of Cp-Ti1 used as a substrate material for coating deposition, LM

The samples for coatings deposition were in the shape of plate with the dimension of 15 mm x 35 mm and a thickness of 0.5 mm. They were ground with the use of sandpaper of 2000 grit and subsequently washed with distilled water and ethanol.

The coatings were deposited on Cp-Ti1 substrates by EPD. A suspension for coating deposition was consisted of 1 g synthetic hydroxyapatite $Ca_5(OH)(PO_4)_3$ (HAp) containing 5 wt % SiO_2 as dopant (Sigma Aldrich, USA) and 100 ml of ethanol. The suspension was ultrasonic treated for 40 minutes and subsequently magnetic stirred (300 rpm) at room temperature for 10 minutes.

EPD was carried out under constant voltage conditions in the range of 20–70 V. Deposition time was 1 minute. The counter electrode was made of austenitic stainless steel AISI316L. The distance between electrodes in the EPD cell was 15 mm. A heat treatment at temperature of 850 ºC during 20 minutes in air was applied on coated substrates (heating rate was 10 ºC/1 min; cooling with furnace).

An influence of applied voltage and deposition time on current density during EPD has been investigated using Tektronix DMM 4040 multimeter. pH values were measured using pH-meter EL20 of Mettler Toledo.

A microstructural characterization of the coated samples was carried out using scanning electron microscopy (SEM). The SEM investigation was performed by FEI Nova NanoSEM 450. The samples were observed directly without any surface preparation. Chemical composition was investigated by energy dispersive X-ray spectroscopy (EDS). The TEM investigation was carried out using a JEOL JEM-2010 ARP microscope. A thin foils for TEM investigation were prepared by dispersing the powder in ethanol and stirring in order to separate agglomerated particles. Finally, a droplet of the stable suspension was placed on a copper grid and dried. Phase identification was performed by selected area electron diffraction (SAED) and X-ray diffractometry (XRD). The XRD (Bragg-Brentano, B-B) and grazing incidence X-ray diffractometry (GIXRD) patterns were recorded using a Panalytical Empyrean DY1061 diffractometer applying Cu-Kα radiation and plan-view specimens.

Coating thickness was measured by contact profilometry. The 5 mm trace length started in the uncoated area and finished on the coating surface. The difference in the recorded height in these areas was equal to coating thickness.

Coatings adhesion to the Cp-Ti1 substrate was measured by the micro-scratch technique using a Micro-Combi Tester (MCT). A Rockwell C spherical diamond stylus with cone apex angle 120° and tip radius 200 μm at the speed (dx/dt) of 5 mm/min was used. Tests were done under continuously increasing load from 0 to 30 N, within the distance of 5 mm. According to the ISO standard [14] the critical loads L_{C1} and L_{C2} that correspond to cohesive and adhesive failures of the coating were determined. Scratches were analyzed using acoustic emission signals and post factum surface examination by light microscopy.

Microhardness and Young's modulus for uncoated and coated alloy were measured on plan-view specimens by a MCT using instrumented indentation technique. Vickers indenter was used and maximum load of 20 mN. At this load penetration depth reached up to 7 μm what is about 30% of coating thickness. The results were analyzed according Oliver and Pharr method [15,16].

The open circuit potential and electrochemical polarization studies of the samples were carried out using a potentiostat Autolab PGSTAT302N. The reference was a saturated calomel electrode and a platinum plate was used as the counter electrode. Ringer's solution was used as the electrolyte for the corrosion study. The chemical composition of the Ringer's solution was: 8.6 g/l NaCl, 0.3 g/l KCl, 0.25 g/l $CaCl_2$. Measurements were performed for pH equal 7.4 and in deaerated solutions at temperature of 37 °C. The polarization test was performed at a scan rate of 1 mV/s from -1.3 V to +1.5 V.

3. Results and discussion

The HAp doped Si powder, later used for coatings deposition, was characterised by electron microscopy methods. The SEM and TEM observation revealed the occurrence of two types of particles: nanocrystalline with diameter up to 90 nm and microcrystalline with size in the range of 0.1 – 1 μm (Fig. 2a,b).

The both types of particles had a spherical shape. SAED patterns analysis confirmed the presence of two phases, calcium dihydroxide hexakis (phosphate) $Ca_{10}(PO_4)_6(OH)_2$ (hexagonal primitive; hp) and an amorphous phase. EDS microanalysis revealed the following mean chemical composition of the powder (in at. %): 39.3 Ca, 25.4 P, 4.6 Si and 30.7 O (Fig. 2c).

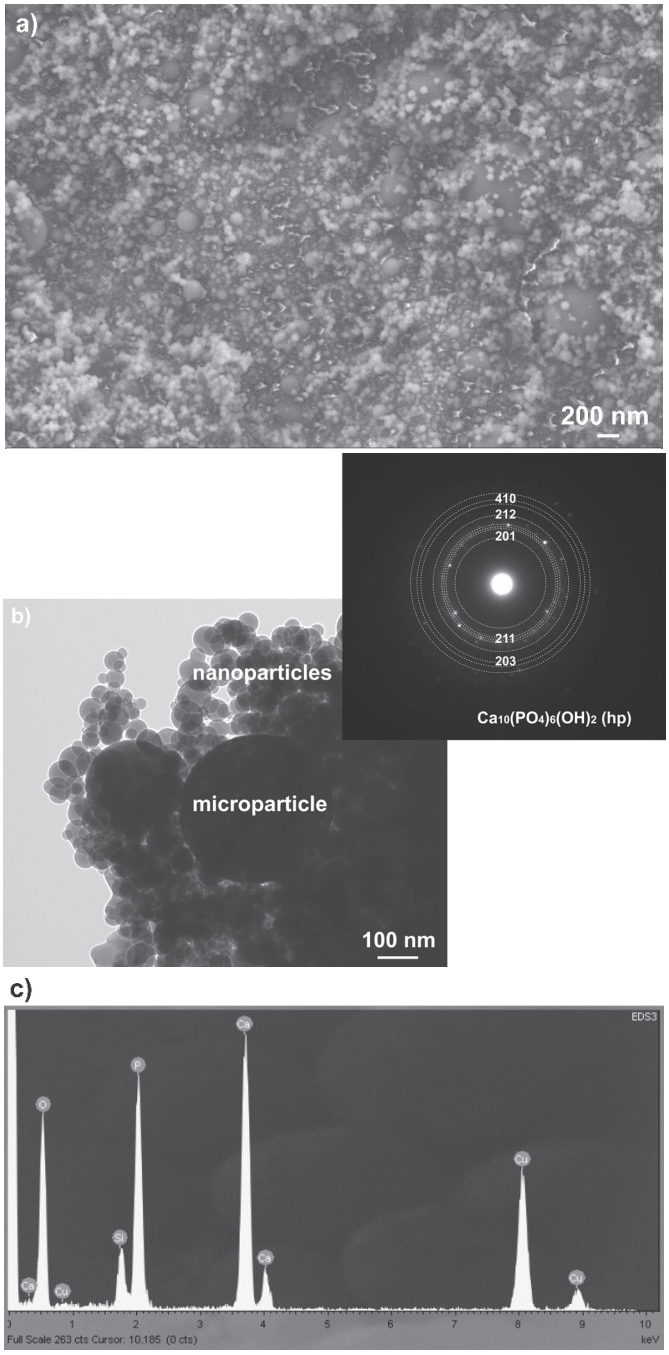

Fig. 2. Microstructure of the hydroxyapatite doped SiO_2 powder used for EPD: a) SEM image, b) TEM image and SAED pattern and its identification as $Ca_{10}(PO_4)_6(OH)_2$ (hp), c) EDS spectrum

During EPD a constant voltage in the range of 20 V – 70 V was applied. Macroscopic images of as-deposited coatings are shown in Figure 3. The best quality, homogeneous coating was obtain at voltage of 60 V during 60 seconds. Thus, such parameters was selected for coatings deposition and subsequently for detailed investigation. The current density was very stable during EPD at 60 V and changed only slightly (Fig. 4a). The deposition yield might be changed by the variation of the deposition time at a constant current density. The deposits weight obtained at different deposition time during EPD with constant voltage of 60 V were investigated. The increase in the deposition time resulted in increasing of deposit weight (Fig. 4b). Nearly linear dependence between deposition time and deposit weight was found. The amount of the deposited material can be controlled by the variation of the deposition time. This founding indicates for an almost constant deposition rate. The obtained deposits were relatively dense and well adherent to the titanium substrate. Their thickness measured by contact profilometry was within 20-25 µm range. Usually coatings were thinner in their periphery.

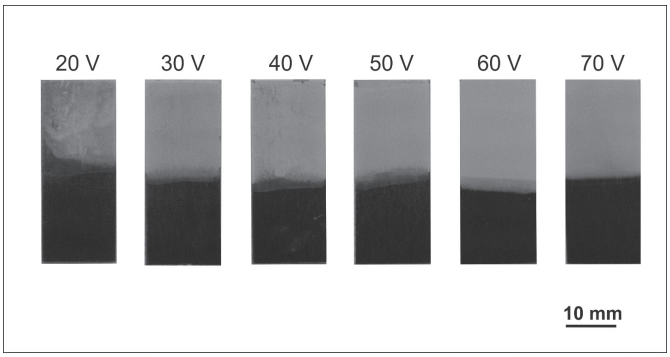

Fig. 3. Macroscopic images of as-deposited SiO_2/HAp coatings on Cp-Ti1 at different voltage and constant deposition time equal to 60 seconds

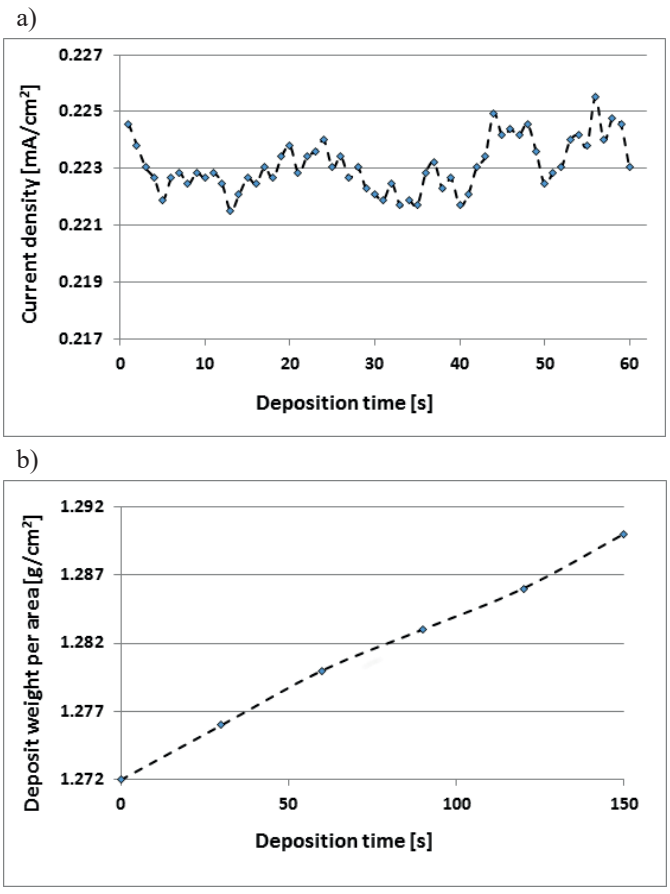

Fig. 4. Typical dependence of deposition time on current density during EPD (a) and weight change of as-deposited coatings at constant voltage of 60 V for different deposition time (b)

It was found during visual inspection and SEM observation that the best quality exhibited the coatings deposited during 60 seconds (Fig. 3). Sporadically small cracks with length of 2 μm -15 μm were observed in the as deposited coatings, as illustrated in Fig. 5a. The microcrystalline HAp particles were uniformly distributed within nanoparticles formed matrix of the coating (Fig. 5b).

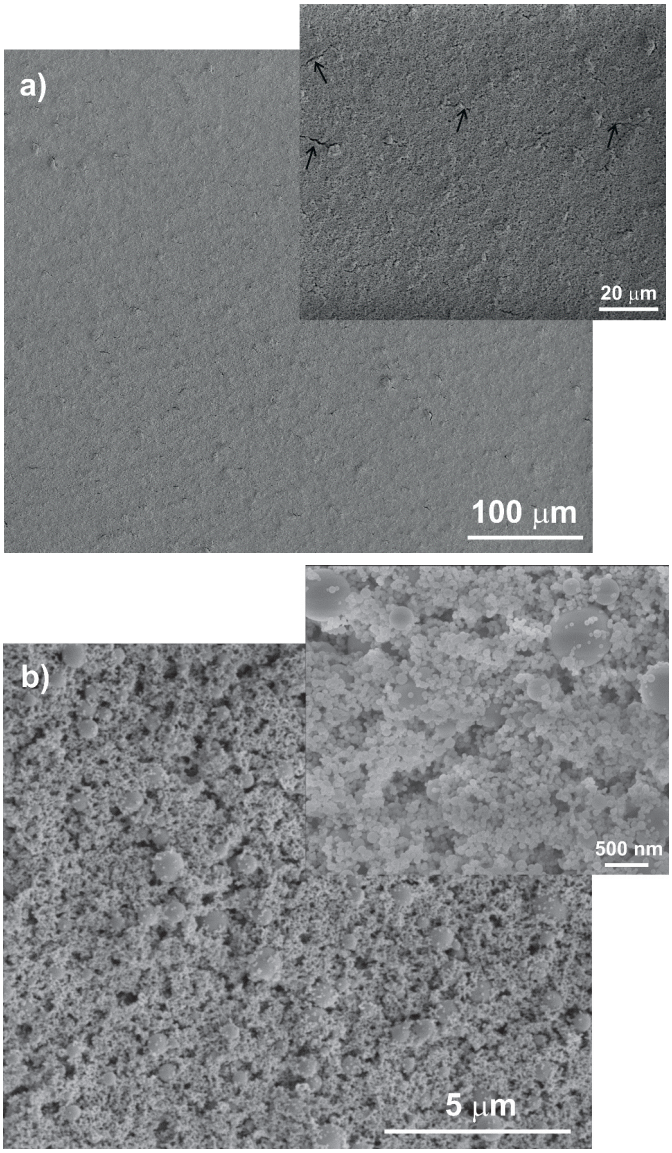

Fig. 5. SEM secondary electron images of the as-deposited coating; plan view specimen. Arrows indicate the microcracks

Thermal treatment is necessary to improve the mechanical properties of HAp. Thus, in order to densify the coatings an annealing of the coated titanium system was carried out at temperature of 850 ºC for 20 minutes. It was found that annealing of as-deposited coatings led to sintering of particles and solid bridges between particles were formed. As a result of drying process, a "dried mud" cracks, characteristic for ceramic coatings, were formed. A degree of microcracking can be observed in Figure 6a. The microcracking could formed during cooling and might be a result of difference in coefficients of thermal expansion (CTE) of the sintered coating and the substrate. The CTE of HAp is higher (approx. 11 x 10^{-6} K^{-1} [17]) than that of the titanium substrate (8.6 $\times 10^{-6}$ K^{-1} [18]). However, the difference is not high and the residual stresses should be minimized. In fact, residual stresses might be introduced by oxidation of the titanium and chemical reactions during annealing at 850 ºC. It is well known [19,20] that titanium has poor oxidation resistance above 300 ºC and titanium oxides quickly form at elevated temperature.

The coatings exhibit high open porosity. The pore diameter distribution along the coating surface was very broad, from few nm up to 1 μm (Fig. 6b). The pores had an irregular geometry. Such porosity was expected, because it is known that particles with larger diameter will produce pores with larger diameter and large difference in particles diameter will produce broad diameter of pores. Thus, the pores size can be controlled by particles diameter. Due to presence of nanoparticles the coatings exhibit very high surface development.

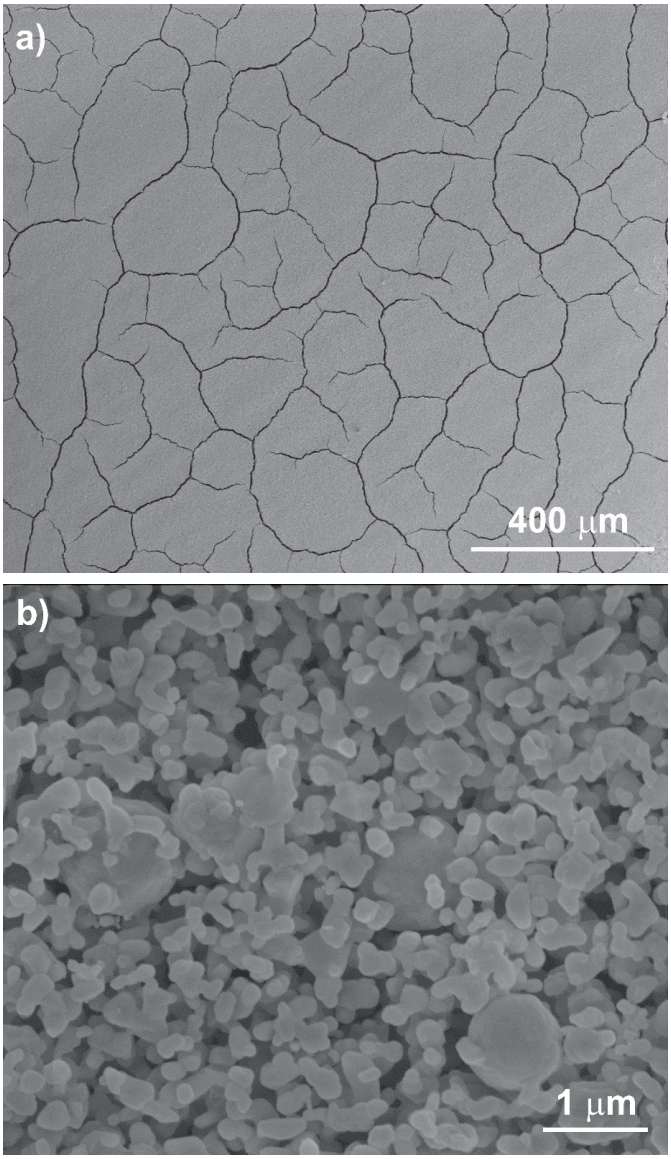

Fig. 6. SEM images of the sintered coating; plan-view specimen

It was observed during SEM and TEM investigation that three types of spherical particles occurred in the coating: HAp with diameter 200 – 600 nm as well as nanocrystalline HA and SiO_2 nanoparticles (with diameter up to 90 nm). The GIXRD investigation of the coating performed at low incidence of 1º

revealed occurrence of peaks of HAp - $Ca_{10}(PO_4)_6(OH)_2$ (hp) (Fig. 7). The presence of small peaks of SiO_2 phase was also observed in GIXRD spectrum. SEM – EDS microanalysis of chemical composition confirmed the presence of Ca, P, Si and O in the coating.

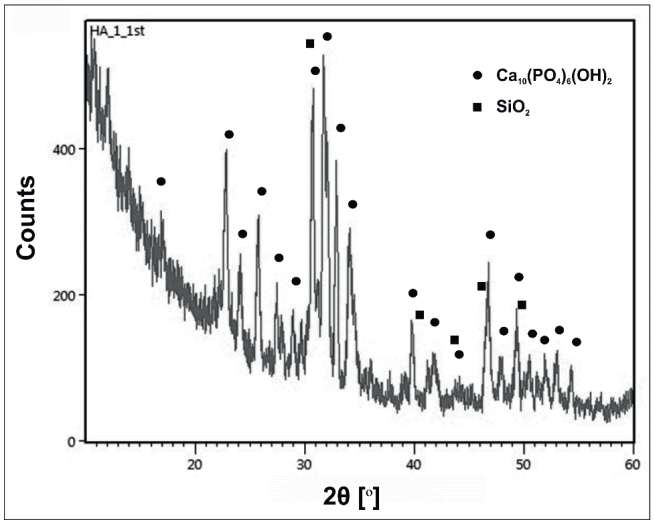

Fig. 7. GIXRD spectrum of the coating performed at low incidence of 1°

The SiO_2/HAp coating exhibits relatively low adhesion to the titanium substrate, typical for porous ceramic. During scratch-tests a cracks and coating delamination from the underlying substrate were observed at 5 N load. The thicker coatings have higher critical loads, what is presented in Ref. [21]. McEntire et al. [22] discussed adhesion of HAp coatings and pointed out huge effect of deposition technique. The better adhesion to metallic substrates than coatings deposited by electrophoresis exhibited these sputtered or applied using Ion Beam Assisted Deposition (IBAD). The mechanical properties and adhesion of HAp coatings can be enhanced by few treatments like deposition of interlayers between HAp and substrate, heat treatment or deposition of coatings with addition of other ceramic particles like SiO_2, TiO_2 .

An average measured coating hardness was 29 ± 15 MPa. The significant scatter of the results is due to great coatings porosity what had a big effect on indentation process. These hardness values are typical for such porous coatings. Although Charitidis et. al. [23] report that hardness of HAp coatings can reach few GPa. It is confirmed by Melero et al. [24] for thick and compact HAp coatings deposited by high-velocity oxy-fuel (HVOF) spraying. They have hardness excided 3 GPa due to introduction into coatings 20% of TiO_2 particles and the low porosity equalled to 5-8%. Whereas it should be pointed the low Young's modulus of the coatings of 1.1 ± 0.4 GPa, similar to the elasticity modulus of cancellous bone.

The influence of coating on corrosion resistance of titanium was investigated in Ringer's solution. Figure 8 shows the evolution of the OCP for the uncoated and SiO_2/HA coated Cp-Ti1 samples. It can be seen that the potential of uncoated and coated titanium was stable in time and equal -0.25 V and -0.06 V (vs SCE), respectively. The observed shift in OCP to positive values for SiO_2/HA coated sample may indicate reduction of the driving force for the corrosion process [25]. Thus, the obtained results suggest that the SiO_2/HAp coating exhibits improved corrosion resistance in comparison to uncoated Cp-Ti1.

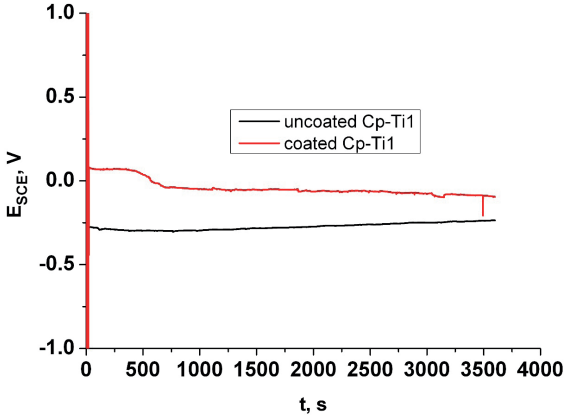

Fig. 8. Evolution of open circuit potential vs. time of tested uncoated and coated Cp-Ti1 in Ringer's solution at temperature of 37 °C

Figure 9 shows the anodic polarization curves for uncoated Cp-Ti1 and coated SiO_2/HAp samples. For the examined materials, similar courses of the obtained curves for the rate of the potential change equaling 1 mV/s was observed. The polarization curves obtained for the tested samples confirmed the results of the open circuit potential tests, which demonstrated that the SiO_2/HAp coating on Cp-Ti1 is characterized by a higher corrosion resistance that the uncoated one. Potentiodynamic polarization curves exhibited a passive range from the potential of the cathodic-anodic transition (-0.06 V) for Cp-Ti1, - 0.28 V for SiO_2/HAp coating for the value equal about 3 V, after which an increase of the current values tooks place. In the case of SiO_2/HAp coating the passive range was minimally longer than in the case of the uncoated titanium. Moreover, for the SiO_2/HAp coating, both the cathode and anode currents were slightly lower than those for the uncoated Cp-Ti1.

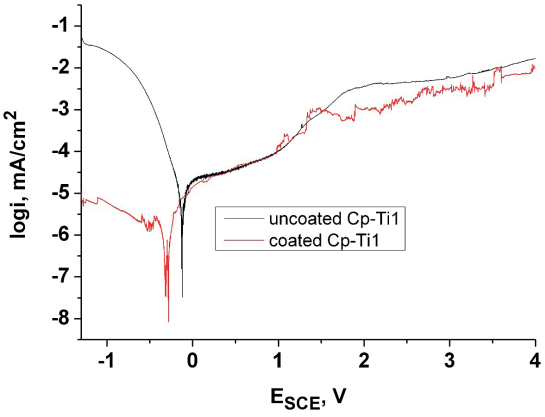

Fig. 9. Anodic polarization curves for Cp-Ti1 and SiO_2/HAp coating on Cp-Ti1 in Ringer's solution at 37 °C and 1 mV/s

4. Summary

The porous composite SiO_2/HAp coatings were produced on Cp-Ti Grade 1 by EPD. SEM images showed that the microstructure of the as-deposited coatings was porous, with some cracks appearing on its surface. Heat treatment of the coated specimen performed at 850 ºC leads to sintering of the particles. The coatings were 20-25 µm thick and consisted of spherical microcrystalline HAp as well as nanocrystalline HAp and SiO_2 nanoparticles. Characteristic "dried mud" cracks were formed within the coatings during drying process after heat treatment.

The coating adhesion to the titanium substrate is typical as for the porous ceramic coatings. In the scratch tests cracks and coating delamination from the underlying substrate was observed at load of 5 N.

The electrochemical measurements showed the results characteristic for materials of a very high corrosion resistance. Comparison of the corrosion characteristics (open circuit potential, polarization curves) of uncoated and coated samples revealed that the overall corrosion resistance property of the SiO_2/HAp coating on Cp-Ti1 was slightly better than that of the uncoated titanium.

Acknowledgments

The study was supported by the AGH-UST (project no 11.11.110.293).

The authors appreciate a valuable contribution of Dr Ł. Cieniek and A. Gruszczyński, MSc (AGH-University of Science and Technology) to SEM investigation.

REFERENCES

[1] Y. Li, C. Yang, H. Zhao, S. Qu, X. Li, Y. Li, Materials **7**, 1709 (2014).
[2] M. Navarro, A. Michiardi, O. Castano, J.A. Planell, J. R. Soc. Interface **5**, 1137 (2008).
[3] V. Oliveira, R.R. Chaves, R. Bertazzoli, R. Caram, Braz. J. Chem. Eng. **15**, 326 (1998).
[4] C.N. Elias, J.H.C. Lima, R. Valiev, M.A. Meyers, JOM **60**, 46 (2008).
[5] M.V. Oliveira, L.C. Pereira, C.A.A. Cairo, Mat. Res. **5**, 269, (2002).
[6] W. Jiang, J. Cheng, D.K. Agrawal, A.P. Malshe, H. Liu, Mater. Res. Soc. Symp. Proc. 1140, 1140-HH03-03 **(**2009).
[7] A.P. Tomsia, M.E. Launey, J.S. Lee, M.H. Mankani, U.G.K. Wegst, E. Saiz, Int J. Oral Maxillofac. Implants **26**, 25 (2011).
[8] J. Dumbleton, M.T. Manley, J. Bone Joint Surg. Am **86**, 2526 (2004).
[9] F. Morks Magdi, A. Kobayashi, Trans. JWRI **25**, 11 (2006).
[10] S. Ghanaati, S.E. Udeabor, M. Barbeck, I. Willershausen, O. Kuenzel, R.A. Sader, C.J. Kirkpatrick, Head Face Med. **9, 1 (**2013).
[11] T. Moskalewicz, M. Kot, S. Seuss, A. Kędzierska, A. Czyrska-Filemonowicz, A.R. Boccaccini, Met. Mater. Int. **21**, 96 *(2015).*
[12] S. Seuss, M. Lehmann, A.R. Boccaccini, Int. J. Mol. Sci. **15**, 12231 (2014).
[13] P. Amrollahi, J.S. Krasinski, R. Vaidyanathan, L. Tayebi, D. Vashaee, Electrophoretic Deposition (EPD): Fundamentals and Applications from Nano- to Micro-Scale Structures, in: Handbook of Nanoelectrochemistry, Springer International Publishing Switzerland (2015).
[14] ISO 20502, "Fine ceramics (advanced ceramics -advanced technical ceramics) - Determination of adhesion of ceramic coatings by scratch testing".
[15] W.C. Oliver, G.M. Pharr, J. Mat. Res. **7**, 1564, (1992).
[16] ISO 14577-1. Metallic materials – instrumented indentation test for hardness and material parameters – Part 1: Test method
[17] G. Willmann, Material properties of hydroxyapatite ceramics, Interceram. **42**, 206 (1993).
[18] D.R. Lide (ed), CRC Handbook of Chemistry and Physics, 84th Edition. CRC Press. Boca Raton, Florida 2003.
[19] G. Lu, S.L. Bernasek, J. Schwartz, Surf. Sci. **458**, 80 (2000).
[20] T. Moskalewicz, B. Wendler, F. Smeacetto, M. Salvo, A. Manescu, A. Czyrska-Filemonowicz, Surf. Coat. Technol. **202**, 5876 (2008).
[21] R. Palanivelu, A. Ruban Kumar, Appl. Surf. Sci. **315**, 372 (2014).
[22] B.J. McEntire, B.S. Bal, M.N. Rahaman, J. Chevalier, G. Pezzotti, J. Eur. Cer. Soc. **35**, 4327 (2015).
[23] C.A. Charitidis, A. Skarmoutsou, A. Tsetsekou, D. Brasinika, D. Tsiourvas, Mat. Sci. Eng. B **178**, 391 (2013).
[24] H. Melero, M. Torrell, J. Fernández, J.R. Gomes, J.M. Guilemany, Wear **305**,8 (2013).
[25] D.J. Blackwood, A.W. Chua, K.H.W. Seah, Corros. Sci. **42**, 481 (2000).